# Supporting Information

## Xie et al. 10.1073/pnas.0912315107

### SI Text

**Tissue Preparation.** *Zbtb20* null mouse embryos and pups were obtained by timed mating of *Zbtb20* heterozygotes, and confirmed by PCR genotyping as described previously (1). The wild-type or heterozygous littermates were used as control. The day on which the vaginal plug was discovered is designated E0.5, and the day of birth P0. To harvest embryo brains, timed-pregnant females were killed, embryos were removed, and brains were dissected out and immersed in Carnoy's fixation (for Nissl staining only) or 4% paraformaldehyde. Mouse pups were anesthetized and perfused transcardially with 4% paraformaldehyde. Brains were fixed overnight in 4% paraformaldehyde, embedded in paraffin, or they were cryoprotected by overnight immersion in 20–30% sucrose before cryosectioning. Paraffin sections (5 μm, for BrdU and Zbtb20) or cryosections (16 μm, for Oct6, Sox5, and active β-catenin) were used for immunostaining.

**cDNA Clones.** The cDNA clones for *Id2* and *ER81* were kindly provided by F. Guillemot (C.U. de Strasbourg, France) (2), and the *Mef2c* clone by Q. Ma (Boston, MA) (3). Other cDNA clones were generated by RT-PCR, using the primers listed in Table S2, and confirmed by DNA sequencing. Antisense riboprobes were transcribed from cDNA clones, labeled with digoxygenin-UTP (Roche), and tested for specificity of hybridization.

**Antibodies.** Mouse anti-Zbtb20 monoclonal antibody clone 9A10 was prepared by peptide immunization (amino acids 720–736 of human Zbtb20; Biosources), and conventional cell fusion and hybridoma selection. The antibody-producing clones were identified by an ELISA-based assay using a GST-Zbtb20 fusion protein as the capture antigen. After multiple rounds of subcloning by limiting dilution, the hybridoma clone 9A10 was established. The monoclonal antibody 9A10 was purified from the ascites using protein-G affinity chromatography. The following primary antibodies were used: anti-Zbtb20 clone 9A10 (1:1,000), anti-Sox5 (1:2,000; Santa Cruz), anti-active β-catenin clone 8E7 (1:1,000; Upstate), anti-Calretinin (1:2,000; Swant), anti-Phospho-Smad1/5/8, anti-Phospho-Smad3, anti-Phospho-p44/42 (Cell Signaling), and anti-Oct6 (1:2,000; Santa Cruz). Secondary antibodies used were from Molecular Probes (1:200).

**Immunohistochemistry.** Tissue sections were incubated overnight at 4 °C with the appropriate primary antibody. After introduction of horseradish peroxidase (HRP) via a secondary antibody, the signal was amplified using a tyramine amplification kit (Perkin-Elmer) according to the manufacturer's instructions, and visualized with Alexa Fluor 594 (Molecular Probes). DAPI was used for nuclear counterstaining. For Zbtb20 and BrdU colabeling, embryos were pulse labeled with BrdU for 1 h by i.p. injection into timed-pregnant female, and coronal forebrain sections were incubated overnight with biotin-coupled sheep anti-BrdU antibody (ab2284; Abcam) and with anti-Zbtb20 monoclonal antibody 9A10. BrdU was then detected by streptavidin-conjugated Alexa Fluor 594; Zbtb20 was detected by a tyramide amplification kit and visualized with Alexa Fluor 488.

**Cell Proliferation and Apoptosis Assays.** For proliferation assays, timed pregnant mice were killed 1 h after i.p. injection of BrdU (100 mg/kg body weight) on the indicated day of embryonic development. Coronal forebrain sections were analyzed for BrdU incorporation using a BrdU In-Situ Detection Kit (BD Pharmingen) as described previously (4). To assess levels of apoptosis, serial coronal forebrain sections (5 μm) were subjected to TUNEL staining following the manufacturer's protocol (Promega). To quantify proliferating and apoptotic cells, equivalent serial coronal sections (four sections for each animal for each genotype, $n = 3–6$) were photographed after immunohistochemistry. The number of labeled cells in each designated area was counted and normalized to the total area to give the base unit in cells/100 $\mu m^2$. Statistical significance was determined using the Student's $t$ test.

**DiI Tracing Study.** Postnatal mice were perfused with 4% paraformaldehyde. The brains were dissected, and small crystals of *FAST* DiI (D7756; Invitrogen), a carbocyanine dye of retrograde and anterograde tracer, were planted into either entorhinal cortex or DG and CA3. The brains were kept in the same fixative solution at 37 °C for either 1 day (for showing mossy fibers) or 10 days and then sectioned at 60 μm thickness with a vibratome. The sections were counterstained with DAPI and immediately photographed under a fluorescence microscope.

**Transcript Profiling.** P2 hippocampi from mice with 129Sv background (N9) were dissected under stereomicroscopy and pooled. Total RNA was subjected to microarray analysis using Affymetrix mouse 430 2.0 chip. GeneChips were washed and stained in the Affymetrix Fluidics Station 400, scanned using the Affymetrix GeneArray Scanner 3000. The data were analyzed with Microarray Suite version 5.0 (MAS 5.0) using Affymetrix default analysis settings and global scaling as normalization method. Differentially expressed transcripts were grouped using gene ontology databases to identify their potential involvement in the relevant biological processes. The array experiments were replicated three times.

**Quantitative RT-PCR.** Real-time RT-PCR was performed in a two-step reaction. First-strand cDNA was synthesized with a SuperScript II RT-PCR Kit (Invitrogen), and the second step was performed in a fluorescent temperature cycler (Mastercycler ep realplex; Eppendorf) with SYBR Green and specific primers for each of the genes. Every plate included 36B4 gene as internal control. Primer sequences are available on request. Results were analyzed with Student's unpaired $t$ test.


1. Sutherland AP, et al. (2009) Zinc finger protein Zbtb20 is essential for postnatal survival and glucose homeostasis. *Mol Cell Biol* 29:2804–2815.
2. Schuurmans C, et al. (2004) Sequential phases of cortical specification involve Neurogenin-dependent and -independent pathways. *EMBO J* 23:2892–2902.
3. Gray PA, et al. (2004) Mouse brain organization revealed through direct genome-scale TF expression analysis. *Science* 306:2255–2257.
4. Xie Z, et al. (2008) Zinc finger protein ZBTB20 is a key repressor of alpha-fetoprotein gene transcription in liver. *Proc Natl Acad Sci USA* 105:10859–10864.

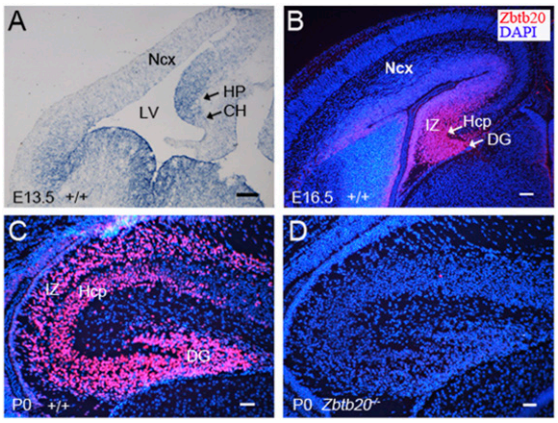


**Fig. S1.** *Zbtb20* expression in the developing hippocampus. (*A–D*) *Zbtb20* in situ hybridization (*A*) and anti-Zbtb20 immunostaining (*B–D*) of coronal sections through wild-type ($^{+/+}$; *A–C*) and *Zbtb20*$^{-/-}$ (*D*) forebrains at E13.5 (*A*), E16.5 (*B*), and P0 (*C* and *D*). (*A*) At E13.5, *Zbtb20* is expressed in the hippocampal primordium (HP), but excluded from the cortical hem (CH) and neocortical neuroepithelium (Ncx). (*B* and *C*) Zbtb20 is observed in the intermediate zone (IZ), the cortical plate (Hcp) of Ammon's horn, and the developing dentate gyrus (DG). (*D*) No anti-Zbtb20 staining is observed in the hippocampus of a *Zbtb20*$^{-/-}$ mutant. (Scale bars: 100 μm for *A*; 50 μm for *B–D*.)

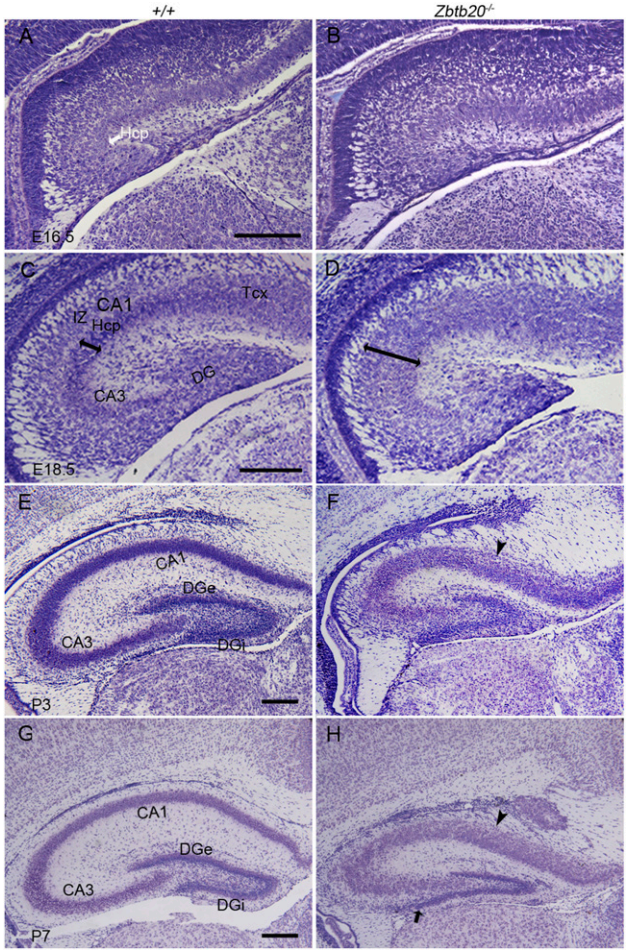


**Fig. S2.** Developing hippocampal morphology in *Zbtb20*$^{-/-}$ mice. (*A* and *B*) Nissl-stained coronal forebrain sections revealed that the *Zbtb20*$^{-/-}$ hippocampal anlage at E16.5 (*B*) is indistinguishable from wild-type (*A*). (*C* and *D*) At E18.5, the wild-type hippocampal anlage is distinguishable from the adjacent transitional neocortex (Tcx) by showing its thinner and more compact Hcp, and its densely populated IZ (*C*). The mutant E18.5 CA1 region displays a comparatively wide and cell-diffuse Hcp, and a thin reticular IZ (*D*). Double-arrow bars indicate Hcp thickness. At P3 (*E* and *F*) and P7 (*G* and *H*), however, the mutant hippocampus (*F* and *H*) displays loosely packed pyramidal neurons in Ammon's horn (arrowheads), as well as a reduction in the size of the DG when compared with wild type (*E* and *G*). Note that in the mutant DG, the DGe is much shorter than DGi accompanied by many neurons abnormally presenting in the DGm (arrow in *H*). Hcp, hippocampal cortical plate; DG, dentate gyrus. DGe, external blade of DG; DGi, internal blade of DG; DGm, DG migratory path. (Scale bars: 200 μm for *A–D*; 400 μm for *E–H*.)

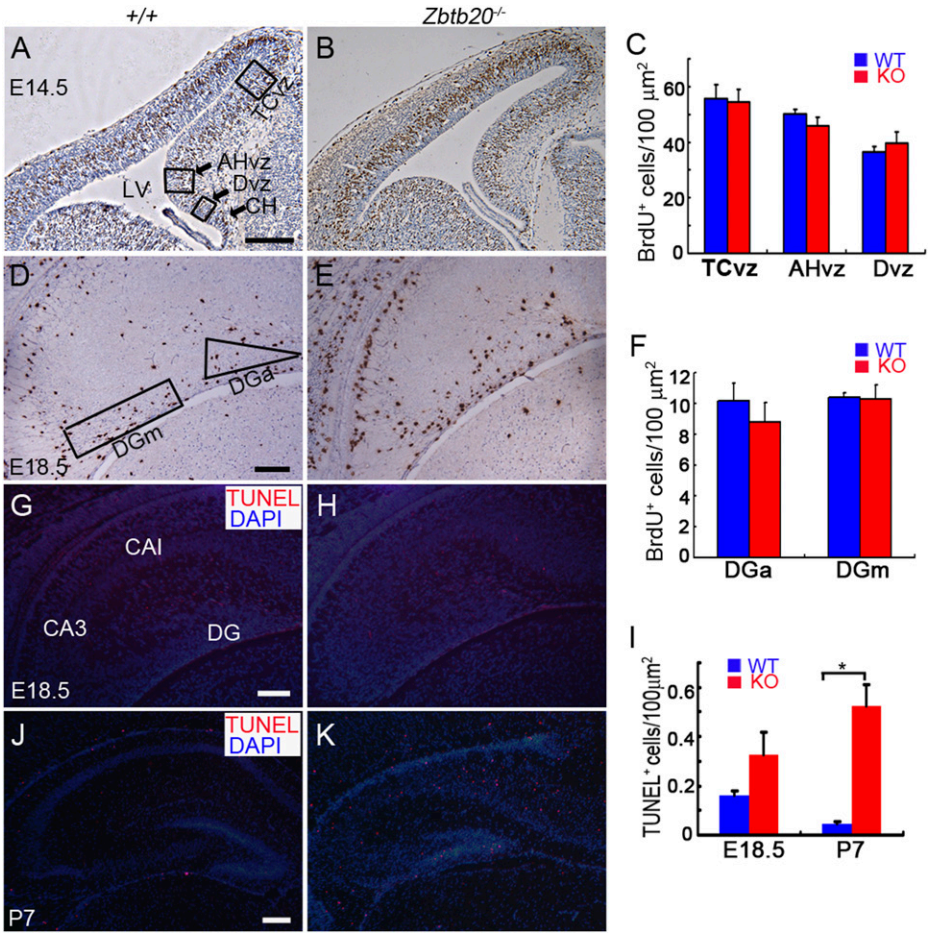


**Fig. S3.** Normal proliferation but increased postnatal apoptosis of the hippocampus from *Zbtb20*$^{-/-}$ mice. (*A–F*) Pregnant female mice carrying wild-type (*A* and *D*) or *Zbtb20*$^{-/-}$ (*B* and *E*) embryos were administered BrdU by i.p. injection at E14.5 (*A* and *B*) or E18.5 (*D* and *E*), and embryonic forebrains were excised 1 h later. Coronal sections were then analyzed for BrdU labeling. (*A*, *B*, *D*, and *E*) Comparable numbers of BrdU$^{+}$ cells (dark brown) are seen in the hippocampal ventricular zone (including AHvz and Dvz), transitional neocortical VZ (TCvz; *A* and *B*), DG migratory path (DGm), and DG anlage (DGa; *D* and *E*) of *Zbtb20*$^{-/-}$ mutants (*B* and *E*) and wild type (*A* and *D*). (*C* and *F*) Quantification of the mean number (±SEM) of BrdU$^{+}$ cells in *A* and *B* and *D* and *E*, respectively. Indicated areas were quantified for BrdU labeling. $P > 0.01$. $n = 3$ in *C*; $n = 5$ in *F*. (*G–K*) Apoptotic cell death detected by TUNEL staining of serial coronal sections of hippocampus. At E18.5, a few TUNEL$^{+}$ cells were detected in the hippocampus of wild-type (*G*) and mutant mice (*H*), with no significant difference between the two. At P7, increased TUNEL$^{+}$ cells were detected in all regions of the mutant hippocampus (*K*) compared with control (*J*). (*I*) Quantification of the mean number (±SEM) of TUNEL$^{+}$ cells in *G* and *H* and *J* and *K*. *$P < 0.0001$, $n = 6$ hippocampi per group. CH, cortical hem; LV, lateral ventricle; AHvz, ventricular zone in Ammon's horn; Dvz, dentate ventricular zone. (Scale bars: 200 μm for *A*, *B*, *J*, and *K*; 100 μm for *D–H*.)

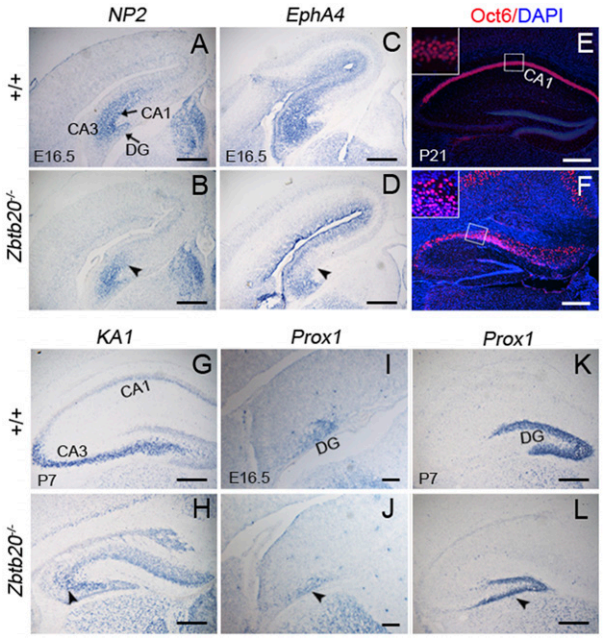


**Fig. S4.** Altered expression pattern of the hippocampus-specific markers in *Zbtb20*$^{-/-}$ hippocampus. (*A–L*) Expression patterns of indicated genes were examined by in situ hybridization or immunohistochemistry on coronal brain sections from wild-type and *Zbtb20*$^{-/-}$ mice. (*A–D*) At E16.5, *NP2* (*A*) and *EphA4* (*C*) mRNA transcripts were present in the wild-type hippocampal primordium (*A* and *C*), but were greatly reduced in the mutant presumptive CA1 (arrowhead in *B* and *D*). (*E* and *F*) At P21, a high level of Oct6 expression (red) was observed in the densely packed wild-type CA1 pyramidal layer (*E*), whereas Oct6$^{+}$ cells were more loosely distributed in the mutant CA1 region (*F*). (*Insets*) High-magnification views of boxed areas. (*G* and *H*) When compared with wild-type control (G), *KA1* expression was relatively weaker in the mutant CA3 (arrowhead in *H*) at P7. (*I–L*) The *Prox1* expression domain in the mutant DG (arrowhead in *J* and *L*) was smaller than that seen in wild-type (*I* and *K*). (Scale bars: 200 μm for *A–D* and *G–L*; 400 μm for *E* and *F*.)

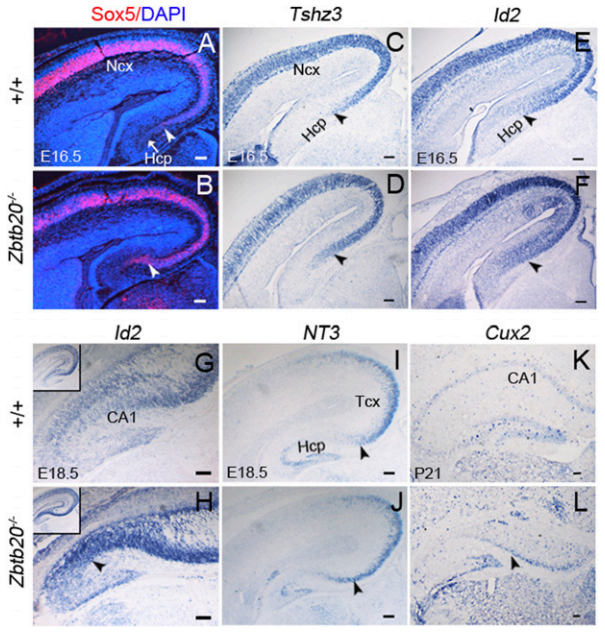


**Fig. S5.** Ventrally expanded expression domain of neocortex-specific markers in *Zbtb20*$^{-/-}$ CA1 region. The expression patterns of indicated genes were examined by in situ hybridization (*C–L*) or immunohistochemistry (*A* and *B*) of coronal forebrain sections from wild-type and *Zbtb20*$^{-/-}$ embryos at E16.5 (*A–F*), E18.5 (*G–J*), and P21 (*K* and *L*). Compared with wild type (*A*, *C*, *E*, *G*, and *I*), the expression domains of Sox5 protein (*B*) as well as *Tshz3* (*D*), *Id2* (*F* and *H*), and *NT3* (*J*) mRNAs expanded more ventrally in *Zbtb20*$^{-/-}$ hippocampi (indicated by arrowheads). In addition, at P21, *Cux2* (a layer II/III/IV marker; *K* and *L*) were ectopically expressed in the upper layer of the mutant CA1 (arrowhead in *L*). Hcp, hippocampal cortical plate; Ncx, neocortex; Tcx, transitional cortex. (Scale bars: 100 μm.)

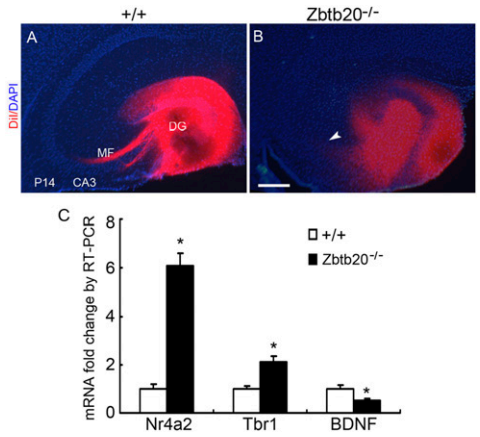


**Fig. S6.** The absence of mossy fibers and altered gene expression in the *Zbtb20*$^{-/-}$ hippocampus. (*A* and *B*) The mossy fibers (MF) were visible in the wild types (*A*) but not in the mutants (*B*, arrowhead) after placing DiI in the DG at P14. (Scale bars: 200 μm.) (*C*) By real-time RT-PCR, the expression levels of *Nr4a2*, *Tbr1*, *and BDNF* were measured in P2 hippocampus with the internal control 36B4 for normalization. $n = 4$, $^*P < 0.01$ vs. wild-type control.

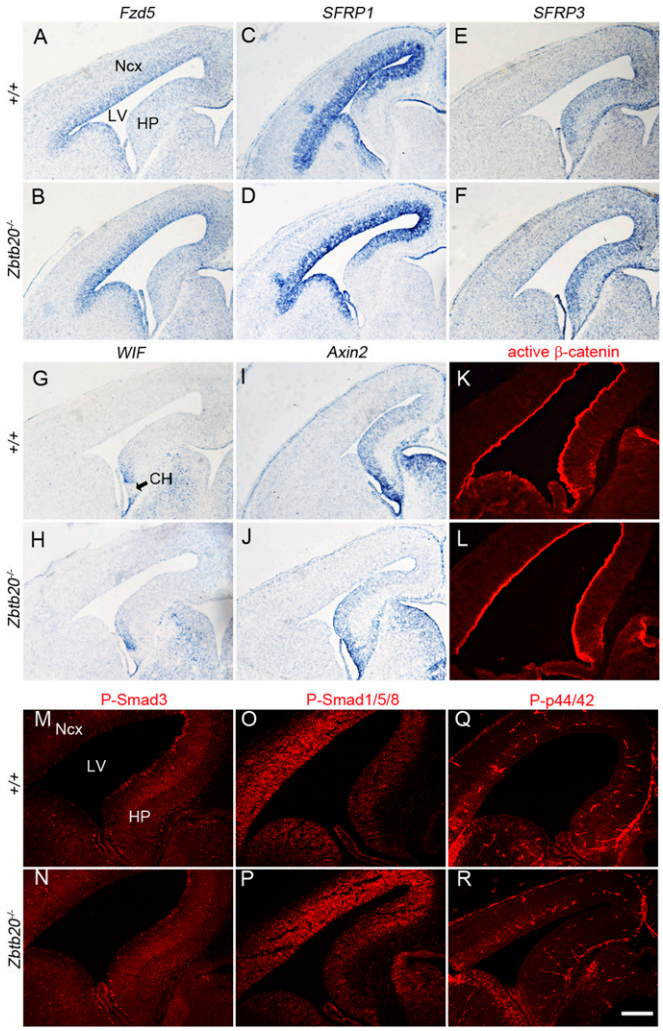


**Fig. S7.** Normal expression and activation of WNT, Smad, and p44/p42 signaling components in *Zbtb20*$^{-/-}$ embryonic forebrain. (*A–J*) In situ hybridization analysis revealed that the indicated genes were expressed comparably in the *Zbtb20*$^{-/-}$ embryonic forebrain relative to the wild type (+/+) at E14.5. (*A–D*) *Fzd5* and *SFRP1* were expressed in the transitional/neocortical VZ. (*E* and *F*) *SFRP3* was expressed in the hippocampal and transitional VZ, but excluded from the neocortex. (*G* and *H*) *Wnt inhibitory factor* (*WIF*) expression was restricted to the hippocampal VZ just dorsal to the cortical hem. (*I* and *J*) *Axin2* was highly expressed in the hem and the adjacent hippocampal VZ. (*K* and *L*) Immunohistochemical analysis of β-catenin activation in wild-type (*K*) and mutant (*L*) E13.5 forebrains by an antibody specifically recognizing activated β-catenin. (*M–R*) Coronal forebrain sections were subjected to immunohistochemistry analysis for the expression of the activated signaling components Phospho-Smad3 (*M* and *N*), Phospho-Smad1/5/8 (O and *P*), and Phospho-p44/42 (*Q* and *R*) in wild-type (+/+) and *Zbtb20*$^{-/-}$ embryos at E14.5. No obvious differences in the expression domains of any of these factors are discernible between wild type and mutants. *Fzd5*, Frizzled 5*; SFRP1*, secreted frizzled-related protein 1; P-Smad3, Phospho-Smad3; P-Smad1/5/8, Phospho-Smad1/5/8; P-p44/42, Phospho-p44/42. (Scale bars: 200 μm.)

**Table S1. Differentially expressed transcripts potentially involved in neuron development, axon guidance, neuron migration, and neuron apoptosis identified by microarray in Zbtb20-KO hippocampus**

| Gene | Gene title | KO/WT fold |
|---|---|---|
| Related with neuron development | | |
| Nr4a2 | Nuclear receptor subfamily 4, group a, member 2 | 4.86 |
| Tshz3 | Teashirt zinc finger homeobox 3 | 4.76 |
| Chl1 | Cell adhesion molecule with homology to l1cam | 2.8 |
| Cntn4 | Contactin 4 | 2.79 |
| NT3 | Neurotrophin 3 | 2.5 |
| Mef2c | Myocyte enhancer factor 2c | 2.37 |
| Id2 | Inhibitor of DNA binding 2 | 2.14 |
| Pbx3 | Pre b-cell leukemia transcription factor 3 | −2 |
| Dlx5 | Distal-less homeobox 5 | −2.01 |
| Sema5a | Semaphorin 5a | −2.01 |
| Zeb2 | Zinc finger e-box binding homeobox 2 | −2.11 |
| Zic2 | Zinc finger protein of the cerebellum 2 | −2.26 |
| Slit2 | Slit homolog 2 (Drosophila) | −2.3 |
| Sema3c | Semaphorin 3c | −2.73 |
| Cck | Cholecystokinin | −2.79 |
| Lhx8 | Lim homeobox protein 8 | −3.92 |
| Zic1 | Zinc finger protein of the cerebellum 1 | −6.99 |
| Related with neuron apoptosis | | |
| Nr4a2 | Nuclear receptor subfamily 4, group a, member 2 | 4.86 |
| Scg2 | Secretogranin ii | 4.13 |
| NT3 | Neurotrophin 3 | 2.5 |
| Igfbp3 | Insulin-like growth factor binding protein 3 | 2.03 |
| Bcl6 | B-cell leukemia/lymphoma 6 | −2.04 |
| Dlx1 | Distal-less homeobox 1 | −2.1 |
| Apoe | Apolipoprotein e | −2.13 |
| Snca | Synuclein, alpha | −2.23 |
| Bdnf | Brain-derived neurotrophic factor | −2.67 |
| Related with neuron migration | | |
| Nr4a2 | Nuclear receptor subfamily 4, group a, member 2 | 4.86 |
| Chl1 | Cell adhesion molecule with homology to l1cam | 2.8 |
| Satb2 | Special at-rich sequence-binding protein 2 | 2.66 |
| Gja1 | Gap junction protein, alpha 1 | −2.04 |
| Onecut2 | One cut domain, family member 2 | −2.11 |
| Cck | Cholecystokinin | −2.79 |
| Related with axon guidance | | |
| Chl1 | Cell adhesion molecule with homology to l1cam | 2.8 |
| NT3 | Neurotrophin 3 | 2.5 |
| Tbr1 | T-box brain gene 1 | 2 |
| Sema5a | Semaphorin 5a | −2.01 |
| Bdnf | Brain-derived neurotrophic factor | −2.67 |

**Table S2. Sequence information for the in situ hybridization RNA probes**

| Gene | GenBank accession no. | Probe position | Probe length, bp | Clone ID |
|---|---|---|---|---|
| Man1α | NM_008548 | 1806–2184 | 379 | 214-3 |
| KA1 | NM_175481 | 1936–3068 | 1133 | 277-5 |
| Prox1 | NM_008937 | 1552–2406 | 855 | 281-2 |
| EphA4 | NM_007936 | 4033–5015 | 983 | 285 |
| EphA6 | NM_007938 | 1902–2697 | 796 | 299-1 |
| MEF2c | NM_025282 | 571–1290 | 720 | |
| ER81 | NM_007960 | 344–1704 | 1361 | |
| Tshz3 | NM_172298 | 2137–3231 | 1095 | 283 |
| NT3 | NM_008742 | 24–820 | 797 | 256 |
| Cux2 | NM_007804 | 3424–4421 | 997 | 262-7 |
| Fzd5 | NM_022721 | 959–1812 | 854 | 269 |
| SFRP1 | NM_013834 | 612–1402 | 791 | 270-6 |
| SFRP3 | NM_011356 | 793–1639 | 847 | 271-1 |
| WIF | NM_011915 | 691–1370 | 680 | 276-1 |
| Axin2 | NM_015732 | 538–1519 | 982 | 279-6 |
| Fibronectin 1 | NM_010233 | 6232–6773 | 542 | 319–6 |